(Received 20 August 2025, Accepted 3 November 2025, Scheduled 7 January 2026)

Calculation of the Permittivity of Lossy Dielectrics Using Cylindrical Cavity Perturbation Technique by Investing in Modified Model of Depolarizing Factor

Khawla Ghorab[1,*], Rawdha Thabet[1], Junwu Tao[2], Mohamed L. Riabi[1], and Tan Hoa Vuong[2]

[1] *Laboratory of Electromagnetic and Telecommunications, University Frères Mentouri Constantine 1, Constantine, Algeria*
[2] *LAPLACE, Toulouse University, CNRS, INPT, UPS, Toulouse, France*

ABSTRACT: To achieve the accurate characterization of a dielectric sample, an improved approach to the cylindrical cavity perturbation technique is proposed, with a particular emphasis on the depolarization factor. The problem arises from the depolarized field within the sample when its height is smaller than that of the cavity, and it depends on the sample's geometry and the orientation of the applied field lines. Two models are examined: the proposed model, based on the resolution of Maxwell's equations, and the ellipsoidal model refined through image theory. The objective is to enhance the accuracy of complex permittivity extraction for lossy dielectric materials. Standard low-loss and high-loss materials (Al_2O_3, Teflon, and SiC) with various shapes (rod, needle, disk, and sphere) are analyzed using HFSS simulations and MATLAB computations. The maximum sample volume is also evaluated for different geometries and material types to ensure accurate permittivity estimation. Low-loss materials generally allow a larger sample volume than high-loss ones, and provide more consistent results for permittivity extraction. Experimental measurements were further performed on disk-shaped polyamide and ceramic samples, demonstrating that the proposed approach provides improved permittivity estimation, particularly for high-loss and disk-shaped dielectric materials.

1. INTRODUCTION

For a considerable amount of research in microwave and radio frequency (RF) engineering, the accurate knowledge of the physical properties of innovative materials is a paramount issue, due to their potential use in various applications, such as filters, antennas, and extremely sensitive RF-circuits [1, 2], with the aim of improving performance. A variety of methods have been applied to the estimation of the permittivity and permeability of materials [3, 4]. One of the most popular, reliable, and simple methods for measuring these properties is the Cavity Perturbation Technique (CPT). This technique serves to characterize homogeneous and isotropic magneto-dielectric materials at microwave frequencies [5]. Mainly, the formulas expressing the electromagnetic perturbation in a resonant cavity are deduced from Maxwell's equations and are based on the measurement of the variation of the resonant frequency and the quality factor Q in the case of a cavity, empty and then loaded by a sample of material [6]. The conventional CPT has a number of limitations that make it susceptible to characterization errors. As such, the sample must be sufficiently small and of a specific shape (rod or bar), and it is usually required that the sample should have the same height as the cavity. Furthermore, it must be placed in a position where the electric field or magnetic field is maximal, depending on whether the complex permittivity or complex permeability is sought [6]. Since certain materials are fragile in nature, difficult to fabricate, particularly in thin forms or very costly, it is necessary to enhance the conventional CPT to facilitate its application. In this context, a number of research works are available in the literature, and most of them have been devoted to the development and optimization of CPT using rectangular resonant cavities [1, 6, 7]. Some studies have employed cylindrical cavities, which not only allow for larger effective volumes but also exhibit higher quality factors than rectangular ones, in addition to simpler fabrication. These distinctive features make cylindrical cavities particularly suitable for the objectives of this work [2]. Improving the performance of the perturbation technique using a cylindrical cavity could enable a more accurate estimation of the complex permittivity of the samples and reduce limitations of the conventional CPT. The accuracy of the calculation to determine the complex permittivity of a given material is dependent on certain critical parameters. It depends significantly on the maximum volume of the material under test (MUT). This volume must be defined to ensure a small resonant frequency shift ($\frac{\delta\omega}{\omega} \leq 10^{-3}$) [8–11]. Therefore, to check the validity of the CPT, it is first necessary to estimate this maximum volume. A second important parameter influencing measurement accuracy is the field polarizing the sample inside the cavity. Successful studies have examined this aspect through the effect of the sample's depolarization factor. When the sample is positioned in the maximum field region of the cavity, a partially polarized field is induced, whose magnitude depends on the sample's dimensions [6]. In other words, the applied field separates the bound charges of the MUT, and this separation generates polarization [6, 10]. The assumption

* Corresponding author: Khawla Ghorab (khawla.ghorab@umc.edu.dz).

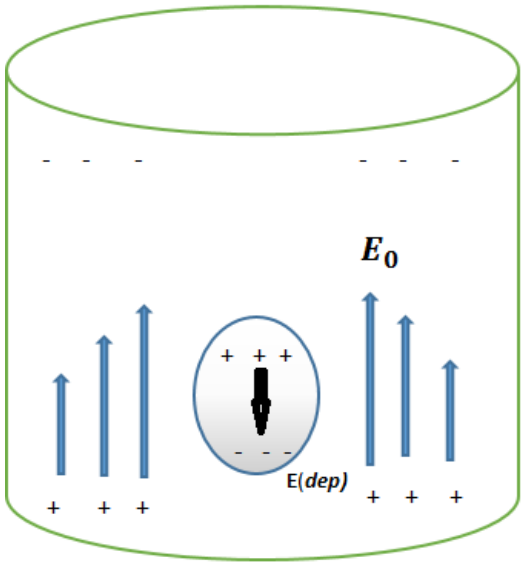

FIGURE 1. Sample polarization with applied electric field in a cylindrical cavity.

also considers the theory of images, where the charges induced on the conducting walls of the cavity produce a series of images of the depolarization field, thereby giving rise to an effective depolarization field [10].

This paper presents an improved CPT approach with modified mathematical formulations, in which the depolarization effect is rigorously analyzed for a dielectric sample placed at the center of a cylindrical cavity, with the sample height smaller than that of the cavity. The depolarizing factor is evaluated using a numerical model derived from the resolution of Maxwell's equations and the widely adopted ellipsoidal model enhanced by image theory [10]. The obtained results are compared with those derived from the solution of Laplace's equation [12].

2. THEORETICAL ANALYSIS BY CONVENTIONAL CPT

When a small sample is inserted into a resonant cavity, it causes a relative shift in the complex resonance frequency $(\delta\omega/\omega)$ giving by [10]:

$$\frac{\delta\omega}{\omega} = t - \frac{(\varepsilon_r^*-1)\,\varepsilon_0 \int_{V_s} \vec{E}\cdot\vec{E}_0^*\,dv + (\mu_r^*-1)\,\mu_0 \int_{V_s} \vec{H}\cdot\vec{H}_0^*\,dv}{\int_{V_c}\left(\vec{D}_0\cdot\vec{E}_0^* + \vec{B}_0\cdot\vec{H}_0^*\right)dv} \tag{1}$$

where $\delta\omega = \omega_s - \omega_0$ is the variation in the complex resonance frequency recorded for the uncharged cavity ω_0 and then charged by the sample ω_s. $\vec{E}$ and $\vec{H}$ are the electric and magnetic fields in the sample; likewise, $\vec{D}_0$, $\vec{E}_0$, $\vec{B}_0$, and $\vec{H}_0$ are the fields in the cavity without a sample. As such, V_c and V_s are the volumes of the cavity and the sample, respectively. The term $\varepsilon_r^* = \varepsilon_r' - j\varepsilon_r''$ is the complex relative permittivity, and $\mu_r^* = \mu_r' - j\mu_r''$ is the complex relative permeability of the sample. ε_0 and μ_0 are the permittivity and permeability of free space, respectively. According to the microwave engineering literature [5, 13], when the inserted sample is nonmagnetic $(\mu_r^* = 1 - j0)$ or is placed at a position where the electric field is maximal, the terms with the magnetic field in Equation (1) vanish. Consequently, the permittivity can be calculated using Equation (2).

$$\frac{\delta\omega}{\omega} = -\frac{(\varepsilon_r^*-1)\int_{V_s}\vec{E}\cdot\vec{E}_0^*\,dv}{2\int_{V_c}\left|\vec{E}_0\right|^2 dv} \tag{2}$$

$(\delta\omega/\omega)$ can be separated into two parts: real, which is the shift in the resonance frequency, and imaginary, which is the change in the quality factor of the cavity:

$$\frac{\delta\omega}{\omega} = \frac{f_s - f_0}{f_0} + j\frac{1}{2}\left(\frac{1}{Q_s} - \frac{1}{Q_0}\right) \tag{3}$$

where f_s is the resonance frequency of the cavity with the sample and f_0 the resonance frequency without the sample. Q_s and Q_0 are the quality factors of the cavity with and without the sample, respectively.

3. PARAMETERS IMPROVING CAVITY PERTURBATION TECHNIQUE

3.1. Depolarization Effect in a Dielectric Sample

The conventional CPT becomes inaccurate when the sample under test has a height smaller than that of the cavity. In this case, the boundary conditions of the sample get changed, and the sample will be partially polarized by the applied electric field $\vec{E}_0$ from the resonant cavity [7, 14]. A new electric field is derived, which is the depolarization field $\vec{E_{ds}}$ (as shown in Figure 1). Hence, the total field $\vec{E_s}$ is the sum of the ideal field from the cavity and the depolarizing one, as reported in previous articles [6, 10]. This approach improves the conventional CPT and adds accuracy in calculating the properties of dielectric materials.

Taking into account the polarization effect, $\vec{E_s}$ inside the sample is written as:

$$\vec{E_s} = \vec{E_0} - \vec{E_{ds}} \tag{4}$$

with

$$\vec{E_{ds}} = \frac{N\,\vec{P_0}}{\varepsilon_0} = N(\varepsilon_r^* - 1)\,\vec{E_s} \tag{5}$$

$\vec{P_0}$ is the polarization.

Consequently,

$$\vec{E_s} = \frac{\vec{E_0}}{1 + N\,(\varepsilon_r^* - 1)} \tag{6}$$

N is the depolarizing factor. It is affected by the geometry and orientation (axial ratio) of the sample with respect to the applied electric field [15, 16]. The formula of N will change due to the change in the symmetries and the edges of different shapes.

In the first approximation, the depolarization factor used is that derived from the ellipsoidal model [15]. For a general ellipsoid with axial dimensions x_1, y_1 (i.e., $x_1 = y_1$) and z_1 (in

the rotation axis), the depolarization factor in the i-th axial direction is given by:

$$N^i = \int_0^\infty \frac{x_1 y_1 z_1 \, du}{2(u+i^2)\sqrt{(u+x_1^2)(u+y_1^2)(u+z_1^2)}}$$
$$i = x_1, \quad y_1, \quad z_1 \quad \text{(Field direction)} \tag{7}$$
$$\text{where}$$
$$N^{x_1} + N^{y_1} + N^{z_1} = 1.$$

3.2. Application of Image Theory and Consideration of Image Dipoles

In fact, the walls of the cylindrical cavity are considered perfect electric conductors (PECs), which creates a series of images of the depolarizing field [10]. Figure 2 shows the image positions of electric dipoles when an electric field is applied in the z-direction; this case is in accordance with an excitation by a TM_{010} mode. Four polarization vectors $\vec{P}_1$, $\vec{P}_2$, $\vec{P}_3$, $\vec{P}_4$ are illustrated, where the direction of any vector is from the negative to the positive charges. This leads to an inversion in the direction of every two successive vectors [6, 7, 10].

The original value of the net dipole is $(P_0 V_0)$ where (V_0) is the volume of the sample; therefore, the nth dipole has a magnitude of polarization equal to $(P_n V_n)$, where (V_n) is the volume of the nth image, as reported in previous research [6, 10]. These vectors can be expressed in function of the original polarization as follows:

$$\vec{P}_1 = -\vec{P}_0 \left(\frac{V_0}{A_1(2H-h)}\right) = -\vec{P}_0 \left(\frac{h}{2H-h}\right),$$
$$\vec{P}_2 = \vec{P}_0 \left(\frac{h}{2H+h}\right), \tag{8}$$
$$\vec{P}_3 = -\vec{P}_0 \left(\frac{h}{4H-h}\right), \quad \vec{P}_4 = \vec{P}_0 \left(\frac{h}{4H+h}\right),$$

A_1 is the area of the cross-section of the sample in the z direction, and h and H are the heights of sample and cavity, respectively. Taking image theory into consideration, the depolarization field is written:

$$\vec{E_{ds}} = \frac{N}{\varepsilon_0} \sum_{n=0}^{\infty} \vec{P_n} \tag{9}$$

From Equation (9), an effective depolarizing factor N_e is derived in the electric field, and $\vec{E}_{ds}$ can be expressed by:

$$\vec{E_{ds}} = \frac{N_e}{\varepsilon_0} \vec{P}_0 \tag{10}$$

where

$$N_e = \frac{N\pi h}{2H} \cot\left(\frac{\pi h}{2H}\right) \tag{11}$$

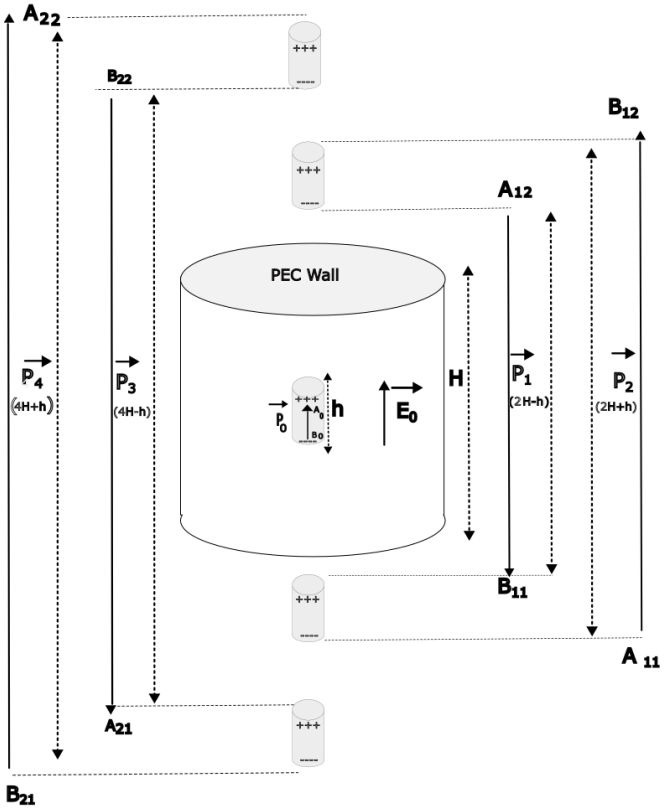

FIGURE 2. Image dipoles for an electric field.

3.3. Numerical Investigation of the Depolarization Factor

The analytical development of the depolarization factor for an ellipsoidal sample was described by Landau and Lifshitz [18], and can also be found in [15] for the case of linear polarization in electrostatic or magnetostatic fields. While several studies have investigated the effective permittivity or permeability of other system geometries using analytical solutions of the electric or magnetic potential, they do not provide explicit analytical expressions for the depolarization factor. These expressions are independent of sample susceptibility and widely used in cylinder or disk-shaped samples. Numerical models have been developed by Venermo and Sihvola in [17] and Chen et al. in [12] to establish corrective functions of a cylinder sample with respect to the ellipsoids as a function of both susceptibility χ and the length to diameter ratio τ. For this, the Laplace equation in magnetostatics [12] or electrostatics [19] has been solved by numerical methods. In the case of a cylinder, both studies show the deviation of the depolarization factor with respect to the ellipsoid approximation, especially for long cylindrical rods with a high susceptibility where significant differences are observed. In this work, we consider a thorough study of the depolarization effect when a sample is placed inside a cylindrical resonant cavity. The solution of perturbed TM_{0np} resonance is governed by the following equation:

$$\iiint_v \frac{1}{\varepsilon_r} \left[\left(\frac{\partial H_\phi^*}{\partial z}\right)\left(\frac{\partial H_\phi}{\partial z}\right)\right.$$

$$+\frac{1}{r^2}\left(\frac{\partial(rH_\phi^*)}{\partial r}\right)\left(\frac{\partial(rH_\phi)}{\partial r}\right)\Bigg]dv$$

$$= k_r^2 \iiint_v |H_\phi|^2\, dv \tag{12}$$

with k_r the propagation constant at resonant frequency.

A finite element method is developed to solve Equation (12). The numerical result for the spatial distribution of $H_\phi(r,z)$ then $E_z(r,z)$ is used to deduce the frequency dependent depolarization factor, referred to here as N_{prop}. To the best of our knowledge, this is the first time that the study of the depolarization factor has been carried out using a rigorous resolution of Maxwell's equations in a resonant cavity.

4. MODIFIED FORMULATION FOR THE ESTIMATION OF ELECTRIC PARAMETERS

For exciting a cylindrical cavity of radius R and height H, TM_{010} mode is the most appropriate. This mode represents a maximum electric field $\vec{E}_0$ in the center of the cavity, vertical according to its height (z-axis). Its components, according to the coordinates (r,ϕ,z), are written as:

$$\begin{aligned} E_{0r} &= 0, \\ E_{0\phi} &= 0, \\ E_{0z} &= E_{0\max} J_0(k_c r) \end{aligned} \tag{13}$$

where J_0 is the Bessel function of the first kind and zero order, and k_c is the cutoff wave vector $k_c = \frac{x_{01}}{R}$, with x_{01} the first root of J_0.

Taking into account the effect of field depolarization, image theory, and the numerical investigation proposed in this work for estimating the depolarizing factor, Equation (2) can be reformuled as:

$$\frac{\delta\omega}{\omega} = -\frac{\varepsilon_r^* - 1}{1 + N_{\text{mod}}\left(\varepsilon_r^* - 1\right)} G_e \tag{14}$$

with

$$G_e = \frac{1}{2}\frac{\displaystyle\int_{V_s} \left|\vec{E}_0\right|^2 dv}{\displaystyle\int_{V_c} \left|\vec{E}_0\right|^2 dv} \tag{15}$$

This allows writing the expressions for permittivity as follows:

$$\varepsilon_r^* = -\frac{C}{CN_{\text{mod}} + G_e} + 1 \tag{16}$$

where $C(=\frac{\delta\omega}{\omega})$ is the relative shift in the complex resonance frequency given in Equation (3), and N_{mod} is the modified depolarizing factor identified as N_e, the (effective depolarizing factor based on the spheroidal model), or N_{prop}, (the proposed depolarizing factor). These formulas allow a more accurate estimation of the permittivity of dielectric materials. They are solved numerically using Matlab.

5. MAXIMUM VOLUME RATIO OF SAMPLE TO CAVITY

The knowledge of the maximum volume of the MUT is important for accurately assessing the complex properties of materials using CPT. In this paper, the maximum sample volume is optimized based on a formulation deduced from Equation (14) for dielectric materials, and by equalizing it to Equation (3) to separate the real and imaginary parts. Different sample shapes were considered (rod ($h = H$), needle, disk, and sphere). To accurately calculate the permittivity and determine whether the MUT introduces a significant volume effect, an allowable frequency shift range $\frac{f_0 - f_s}{f_0} \leq 10^{-3}$ is considered according to experiment work of [8]. It should be noted that the lower limit of the measurable frequency shift is practically constrained by the cavity quality factor. The parameter $\frac{1}{Q_0}$ serves as a practical detectability criterion, since it defines the frequency resolution of the resonator system. For a cylindrical cavity, with radius R and height H, operating in the TM_{010} mode, and for a sample placed in its center, by equalizing the real parts of Equations (3) and (14), the frequency shift range is obtained as follows:

$$\begin{aligned} &\frac{f_0 - f_s}{f_0} \\ &= \frac{1}{2}\frac{V_s}{V_c} A \frac{N_{\text{mod}}\left(\varepsilon_r'^2 + \varepsilon_r''^2\right) + \varepsilon_r'\left(1 - 2N_{\text{mod}}\right) + N_{\text{mod}} - 1}{\left(1 + N_{\text{mod}}\varepsilon_r' - N_{\text{mod}}\right)^2 + \left(N_{\text{mod}}\varepsilon_r''\right)^2} \\ &\leq 10^{-3} \end{aligned} \tag{17}$$

where, for a cylindrical shape of the sample, A is given by:

$$A = \frac{J_1^2(k_c a) + J_0^2(k_c a)}{J_1^2(x_{01})} \tag{18}$$

J_1 is the Bessel function of the first kind and first order, and a is the radius of the cylindrical sample.

Therefore, the ratio of the maximum sample volume to the volume of the cavity is given by:

$$\begin{aligned} &\left(\frac{V_s}{V_c}\right)_{\max} \\ &= \frac{\left(1 + N_{\text{mod}}\varepsilon_r' - N_{\text{mod}}\right)^2 + \left(N_{\text{mod}}\varepsilon_r''\right)^2}{500A\left[N_{\text{mod}}\left(\varepsilon_r'^2 + \varepsilon_r''^2\right) + \varepsilon_r'\left(1 - 2N_{\text{mod}}\right) + N_{\text{mod}} - 1\right]} \end{aligned} \tag{19}$$

Three shapes of the dielectric sample are discussed: rod, sphere, and thin disk.

Figure 3 shows the variation of the volume ratio $(\frac{V_s}{V_c})_{\max}$ as function of the permittivity for different shapes. In the case of a rod with $h = H$, $(\frac{V_s}{V_c})_{\max}$ depends only on the relative dielectric constant ε_r', and the ratio decreases as ε_r' increases (see Figure 3(a)). For the values of ε_r' less than 1.7, $(\frac{V_s}{V_c})_{\max}$ decays rapidly while its variation becomes slower for higher increasing values. In the case of a thin disk, the maximum volume ratio depends on both the relative dielectric constant and the loss factor. Figure 3(b) shows that this ratio decreases rapidly in the intervals of 1 to 2.5 for ε_r' and 1 to 1.5 for ε_r''. A much

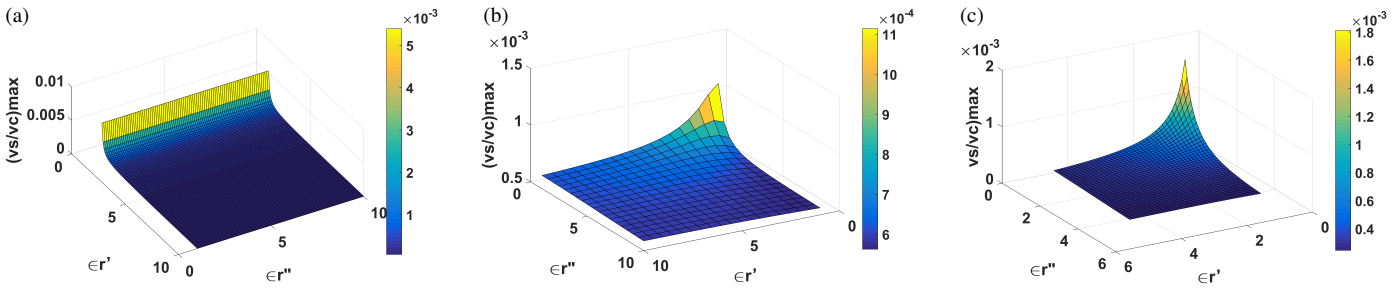

FIGURE 3. $(\frac{V_s}{V_c})_{\max}$ as a function of the permittivity for (a) rod, (b) disk, (c) sphere.

TABLE 1. Comparison between maximum volume ratios, $(V_s/V_c)_{\max}$, of sample to circular cavity and sample to rectangular cavity for dielectric materials, using CPT with the ellipsoid model of the depolarizing factor (N).

Shape of the sample	Materials							
	Al_2O_3					SiC		
	a/R	$h/2a$	Cylindrical cavity	Rectangular cavity [6]	Rate of increase	Cylindrical cavity	Rectangular cavity [6]	Rate of increase
Rod	0.009	500	6.82445×10^{-5}	6.32961×10^{-5}	+ 7.82%	2.10079×10^{-5}	1.94846×10^{-5}	+ 7.82%
Needle	0.009	30	6.95572×10^{-5}	6.45136×10^{-5}	+ 7.82%	2.09481×10^{-5}	1.94292×10^{-5}	+ 7.82%
Sphere	0.07	1	2.49669×10^{-4}	2.29958×10^{-4}	+ 8.57%	1.91196×10^{-4}	1.76101×10^{-4}	+8.57%
Thick disk	0.15	0.2	4.87290×10^{-4}	4.37542×10^{-4}	+ 11.37%	4.26987×10^{-4}	3.83396×10^{-4}	+11.37%
Thin disk	0.15	0.01	6.18545×10^{-4}	5.55398×10^{-4}	+ 11.37%	5.58177×10^{-4}	5.01193×10^{-4}	+11.37%

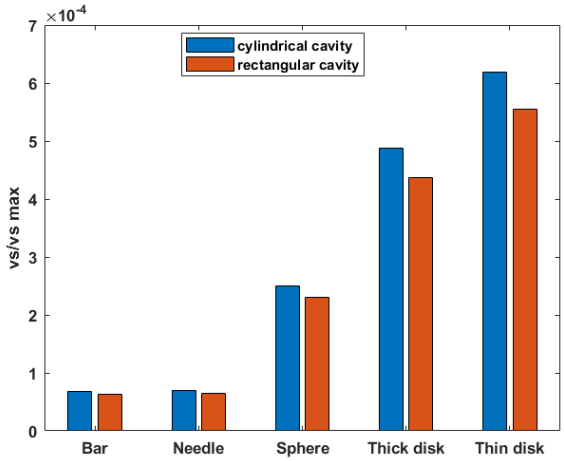

FIGURE 4. Maximum volume ratios of Al_2O_3 sample in circular and rectangular cavities, with different geometries.

slower decrease is observed in the higher intervals; for example, when $\varepsilon_r' = 10$ and $\varepsilon_r'' = 10$, the volume ratio tends towards 0.00057062. Regarding the graph in Figure 3(c), which is related to the sphere case, there is a very rapid decrease in $(\frac{V_s}{V_c})_{\max}$ with the increase of ε_r' and ε_r'' for values of the two parameters, ranging from 1 to 1.4. The decreasing pace of the curve becomes slower for larger values. Table 1 shows the simulation results for 2 types of dielectric materials: a low-loss material, Al_2O_3 ($\varepsilon_r^* = 8.90 - 0.004i$ with $\tan\delta = 0.000449$) at 2.45 GHz [20], and a high-loss material, SiC ($\varepsilon_r^* = 26.66$–27.99i with $\tan\delta = 1.05$) at 2.45 GHz [21]. The simulation results are obtained using the CPT with the ellipsoidal model of the depolarizing factor (N factor). The rate of increase in the volume ratio is then evaluated by comparing these results with those from a previous study involving a rectangular perturbed resonant cavity [6].

As reported in Table 1 and Figure 4, the maximum volume ratio is greater for the circular cavity, regardless of the dielectric material or its geometry. The rate of increase follows the ratio $\frac{a}{R}$ for both types of dielectrics. This improvement in volume ratio offers more flexibility in choosing the sample size. For low-loss materials, with a low dielectric constant, such as Teflon (ε_r^*=2.1-j0.001), the sample volume is even larger across all the studied geometries [11]. Moreover, considering the increased rate of the ratio $(\frac{V_s}{V_c})_{\max}$, the order of the geometries for a given material is: thin disk > thick disk > sphere > needle > rod.

6. NUMERICAL ESTIMATION OF COMPLEX PERMITTIVITY USING FULL-WAVE ELECTROMAGNETIC SIMULATION

The modified cavity perturbation technique (CPT), employing the two depolarizing factor models (N_e and N_{prop}) developed in Section 4, is applied to extract the complex permittivity of samples with various geometries (rod or needle, disk, and sphere) and dimensions. The samples are loaded into a cylindrical cavity ($R = 46.75$ mm, $H = 33.9$ mm), operating in the TM_{010} mode at 2.451470 GHz. Electromagnetic simulations were performed using ANSYS HFSS and COMSOL Multiphysics, both based on the finite element method (FEM) to solve Maxwell's equations in the frequency domain. Table 2 presents the extracted complex permittivity values for Teflon, alumina (Al_2O_3), and silicon carbide (SiC) obtained using the

TABLE 2. Permittivity of teflon, Al_2O_3 and SiC obtained by the modified CPT based on the spheroidal model.

Sample shape	sample sizes (mm)	$h/2a$	$\frac{f_0-f_s}{f_0}$	Classical CPT, using N [15]	Relative error		Modified CPT, using N_e	Relative error	
					Real part	Imaginary part		Real part	Imaginary part
Teflon									
Needle	$a = 0.9; h = 18$	10	$3.8543 * 10^{-4}$	$2.0795 - 0.00098i$	0.98%	2.34%	$2.0737 - 0.00097i$	1.25%	3.37%
Sphere	$a = 3.5; h = 7$	1	$1.1514 * 10^{-3}$	$2.0795 - 0.3462i$	0.98%	34518.64%	$2.0673 - 0.3375i$	1.56%	33654.73%
Disk	$a = 7; h = 2.5$	0.178	$1.8685 * 10^{-3}$	$2.2238 - 0.0012i$	5.89%	25.34%	$2.2186 - 0.0012i$	5.65%	24.28%
Al_2O_3									
Rod ($h = H$)	$a = 0.42075$; $h = 33.9$	40.285	$1.1922 * 10^{-3}$	$8.9343 - 0.0041i$	0.39%	1.20%	$8.9343 - 0.0041i$	0.39%	1.20%
Needle	$a = 0.8; h = 29$	18.125	$3.3801 * 10^{-3}$	$8.7214 - 0.0039i$	2.01%	2.13%	$8.4088 - 0.0036i$	5.52%	9.89%
	$a = 0.7; h = 15$	10.71	$1.2248 * 10^{-3}$	$8.5771 - 0.0038i$	3.63%	4.83%	$8.4067 - 0.0036i$	5.54%	9.06%
SiC									
Needle	$a = 0.09; h = 7$	38.89	$3.5039 * 10^{-5}$	$25.7597 - 25.3382i$	3.38%	9.47%	$25.7618 - 25.24i$	3.37%	9.83%

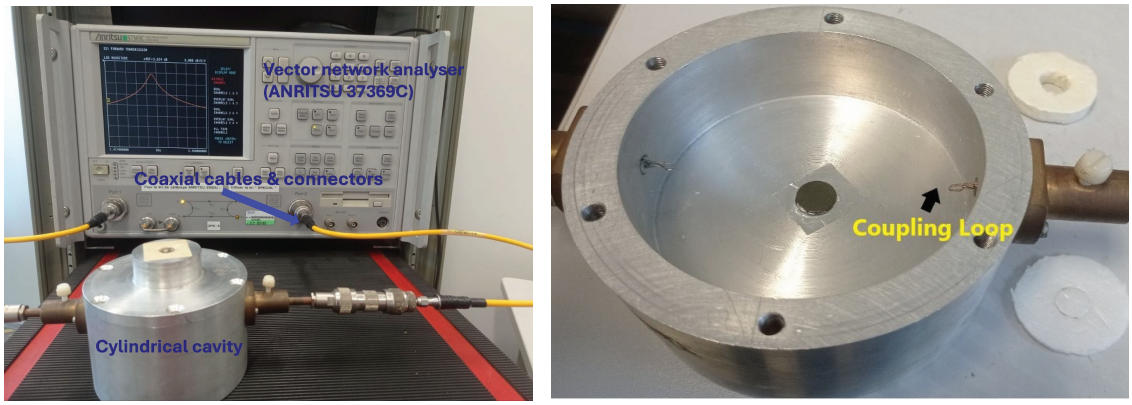

FIGURE 5. Photograph of the cavity used for the experimental measurements.

CPT based on the ellipsoidal depolarization factor, considering both the classical N and modified (N_e) models. The results show that including the image effect in the modified CPT does not significantly improve the calculation accuracy or reduce the relative error. It is also observed that the accuracy decreases as the height-to-diameter ratio ($\frac{h}{2a}$) decreases. The error becomes more pronounced for disk-shaped samples, even for low-loss dielectrics. For high-loss materials such as SiC, satisfactory results are obtained for a needle-shaped sample ($\frac{h}{2a} \gg 1$). In contrast, the spherical sample exhibits less accurate estimation of dielectric losses. The permittivity values of the tested materials were also estimated using the CPT based on the proposed depolarization factor model, in comparison with Chen's model [12]. The results, summarized in Table 3, indicate that both models provide comparable estimations for low-loss dielectrics, with a noticeable reduction in the overall error compared with the modified ellipsoidal model. Moreover, the accuracy in evaluating dielectric losses is significantly improved, particularly for the Teflon disk. Conversely, Chen's model appears inadequate for SiC, which exhibits high dielectric losses. It is worth noting that the accuracy of the results is constrained by the maximum frequency shift, which must remain on the order of 10^{-3} to allow for precise permittivity determination.

7. EXPERIMENTAL TECHNIQUE AND MEASUREMENT RESULTS

7.1. Experimental Technique

The experimental setup consists of an aluminum cylindrical cavity, fabricated at the LAPLACE laboratory and connected to a network analyzer (ANRITSU 37369C) (Figure 5). With a height of 33.9 mm and a diameter of 93.5 mm, the cavity operates in the fundamental TM_{010} resonance mode, corresponding to an empty-cavity resonance frequency of 2.45432 GHz. The resonance frequency and quality factor were determined using the reflection-transmission method. For practical implementation, only the transmission coefficient (S_{21}) was considered, since the intrinsic quality factor of the cavity can be directly derived from the S_{21} measurement, in contrast to the use of the reflection parameter (S_{11}) [23].

TABLE 3. Permittivity of Teflon, Al_2O_3 and SiC obtained by the modified CPT using the proposed model and the spheroidal model, in comparison with the CHEN model.

Sample shape	sample sizes (mm)	$h/2a$	$\frac{f_0-f_s}{f_0}$	Modified CPT, using N_e	Relative error		CPT using Chen model [12]	Relative error		CPT with N_{prop}	Relative error	
					Real part	Imaginary part		Real part	Imaginary part		Real part	imaginary part
Teflon												
Needle	$a=0.9$; $h=18$	10	$3.8543*10^{-4}$	$2.0737-0.00097i$	1.25%	3.37%	$2.0869-0.00099i$	0.62%	1.00%	$2.0925-0.0010i$	0.357%	0.00%
Disk	$a=7$; $h=2.5$	0.178	$1.8685*10^{-3}$	$2.2186-0.0012i$	5.65%	24.28%	$2.1018-0.0010i$	0.09%	2.00%	$2.0784-0.00097i$	1.03%	3.00%
Al_2O_3												
Needle	$a=0.8$; $h=29$	18.125	$3.3801*10^{-3}$	$8.4088-0.0036i$	5.52%	9.89%	$8.5053-0.0037i$	4.43%	7.52%	$8.5861-0.0038i$	3.53%	5.00%
	$a=0.7$; $h=15$	10.71	$1.2247*10^{-3}$	$8.4067-0.0036i$	5.54%	9.07%	$8.7049-0.0039i$	2.19%	1.60%	$8.9628-0.0042i$	0.71%	5.00%
SiC												
Needle	$a=0.09$; $h=7$	38.89	$3.5039*10^{-5}$	$25.7618-25.24i$	3.37%	9.83%	$-4.6402-0.6508i$			$25.4205-28.8905i$	4.65%	3.22%

TABLE 4. Permittivity of a polyamide sample derived from experimental data (average $\varepsilon_r \approx 2.8$ at 2.45 GHz; cavity dimensions: $R = 46.75$ mm, $H = 33.9$ mm).

Sample	Disk sizes (mm)	$h/2a$	$\frac{f_0-f_s}{f_0}$	Modified CPT using N_e	Relative error	CPT using Chen [12]	Relative error	CPT using proposed model N_{prop}	Relative error
Polyamide	Disk 1 ($a=6.3$, $h=6.9$)	0.548	6.9396×10^{-3}	$3.0883-0.0746i$	10.30%	$2.8080-0.0559i$	0.29%	$2.8206-0.0567i$	0.74%

7.2. Measurement of Polyamide Cylindrical Sample

Curtis [24] investigated the dielectric properties of polyamide disks over a temperature range from 100°C to 175°C and for frequencies spanning 50 Hz to 10 MHz. The relative permittivity values obtained at 23°C are illustrated in Figure 6, showing that the relative permittivity decreases with increasing frequency. At 10 MHz, the complex permittivity of the dielectric is $\varepsilon_r^* = 3.009 - 0.0629i$. The measurement of a polyamide disk with a diameter of 12.6 ± 0.1 mm and a height of 6.9 ± 0.1 mm was made at 23°C in LAPLACE laboratory using our experiment setup. The extracted permittivity results are summarized in Table 4, where a comparison among different depolarizing factor models is presented. A dielectric constant value of 2.8 was obtained at 2.45 GHz using both Chen's model and the proposed model, corresponding to a relative error below 1%. This result is in good agreement with the reference value of approximately 2.8 reported for this polymer around 1 GHz.

7.3. Measurement of Ceramic Disks

Two disk-shaped dielectric samples were measured. They had diameters of 10 mm ± 0.025 mm, with heights of 2 mm ± 0.01 mm and 4 mm ± 0.01 mm, respectively. These specimens are part of a batch of high-loss ceramics that had previously been investigated using several alternative techniques [19]. Based on inverse modeling through measurement-HFSS simulation comparison, the relative permittivity at 25°C was determined to be 14.0 ± 0.490, with a corresponding loss tangent of 0.18 ± 0.024. Figure 7 compares the measured transmission coefficient as a function of frequency, both in the absence of a sample and with either disk 1 or disk 2 placed at the center of the cavity. The resonance frequency shift is more pronounced for disk 2 than for disk 1, indicating a stronger perturbation due to the doubled sample volume. We also investigated the influence of sample positioning accuracy within the cavity on the measurement results and, consequently, on the extracted complex permittivities. This issue was discussed in [22]. Figure 8 illustrates the case of non-centred sample, for which the expansion of the numerator in Equation (15) becomes dependent on a coordinate transformation (r', ϕ', z), expressed in terms of the cylindrical coordinates (r, ϕ, z) such that:

$$\phi' = \arctan\left(\frac{-r\sin\phi}{D - r\cos\phi}\right) \tag{20}$$

$$r' = \frac{r\sin\phi}{\sin\left(\arctan\left(\frac{-r\sin\phi}{D-r\cos\phi}\right)\right)} \tag{21}$$

Measurements were performed with the two samples positioned at distances D of 5 mm and 10 mm from the center of

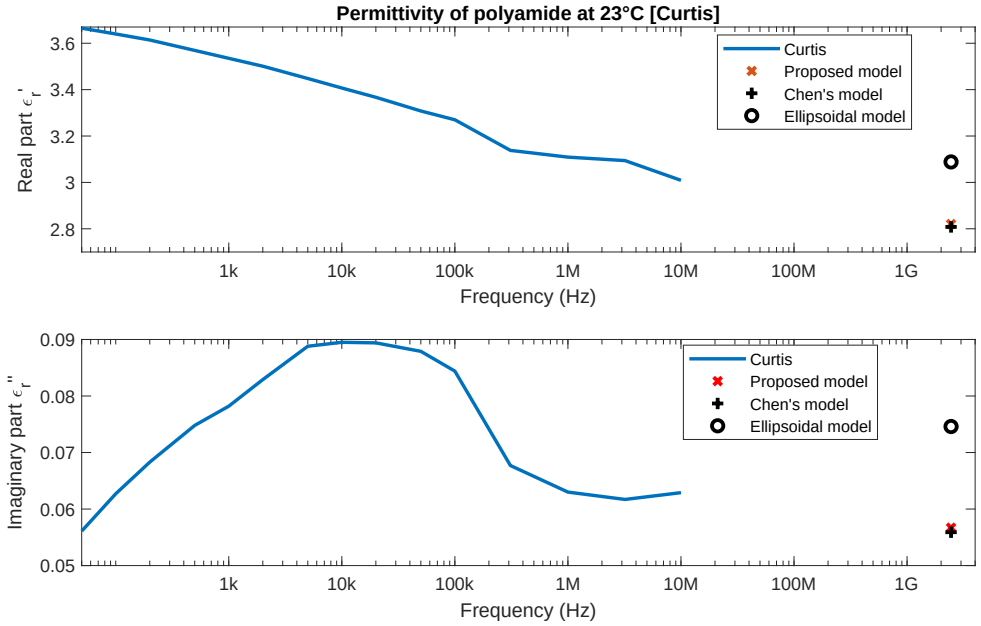

FIGURE 6. Relative permittivity of polyamide at 23°C as a function of frequency according to Curtis [24], and at 2.45 GHz according to the present work.

TABLE 5. Permittivity of a ceramic sample derived from experimental data at three positions from the center of cavity (average $\varepsilon_r^* \approx 14 - 2.52i$; cavity dimensions: $R = 46.75$ mm, $H = 33.9$ mm).

Sample sizes (mm)	$h/2a$	Position	$\frac{f_0 - f_s}{f_0}$	Modified CPT, using N_e	Relative error	CPT using Chen model [12]	Relative error	CPT using proposed model N_{prop}	Relative error
Disk 1	0.2	1 ($D = 0$ mm)	0.0016	$1.8951 - 12.9877i$	86.46%	$6.9516 - 3.8507i$	50.35%	$5.7285 - 2.0288i$	59.08%
($a = 5$,		2 ($D = 5$ mm)	0.0017	$-13.2368 - 3.8209i$		$19.4742 - 6.8194i$	39.10%	$9.8782 - 1.4304i$	29.44%
$h = 2$)		3 ($D = 10$ mm)	0.0017	$-7.9232 - 3.3595i$		$10.4323 - 23.2307i$	25.48%	$11.5184 - 5.0693i$	17.73%
Disk 2	0.4	1 ($D = 0$ mm)	0.0052	$-7.6478 - 1.6326i$		$-15.2406 - 41.0061i$		$20.6761 - 10.4734i$	47.69%
($a = 5$,		2 ($D = 5$ mm)	0.0052	$-6.3573 - 2.3732i$		$-9.0530 - 20.1716i$		$12.9114 - 16.5703i$	7.77%
$h = 4$)		3 ($D = 10$ mm)	0.0047	$-6.3785 - 1.9111i$		$-13.4155 - 20.0174i$		$15.5632 - 19.4037i$	11.17%

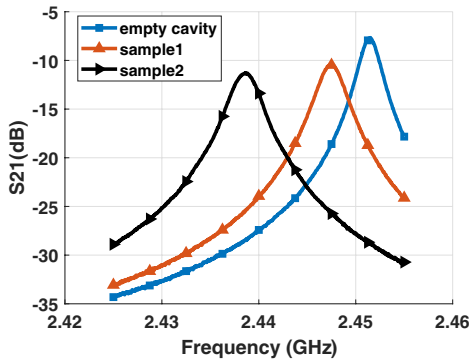

FIGURE 7. S_{21} parameters of the cavity loaded with a centered sample (position 1 at 0 mm) compared with those of the empty cavity.

the cavity. The results are presented in Figure 9 and Figure 10. The change in sample position affects the cavity resonance frequency more significantly in the case of disk 2.

As shown previously, the CPT based on the proposed depolarization factor model or Chen's model achieves satisfactory results for disk-shaped, low-loss materials compared to the ellipsoidal model. It is also observed that Chen's model yields good results for disk-shaped, medium-loss materials (such as polyamide) but becomes unsuitable for high-loss dielectrics (such as SiC), whereas the proposed model maintains good accuracy for both material types.

Table 5 reports the estimated permittivity values of the high-loss ceramic (loss tangent ≈ 0.18) in Disk 1 and Disk 2 configurations, evaluated at the positions indicated above. The modified CPT employing the ellipsoidal model does not provide an accurate estimation of the complex permittivity, while the proposed model yields a better approximation, especially for the thin disk.

Furthermore, the proposed model produces results that are significantly better than those of Chen's model, particularly when estimating the loss factor of a thin disk in a non-centered position. The results obtained using Chen's model become erroneous when the disk thickness is doubled. It is also observed that increasing the displacement of the sample from the cavity center leads to a significant rise in dielectric losses, particularly when the thickness increases.

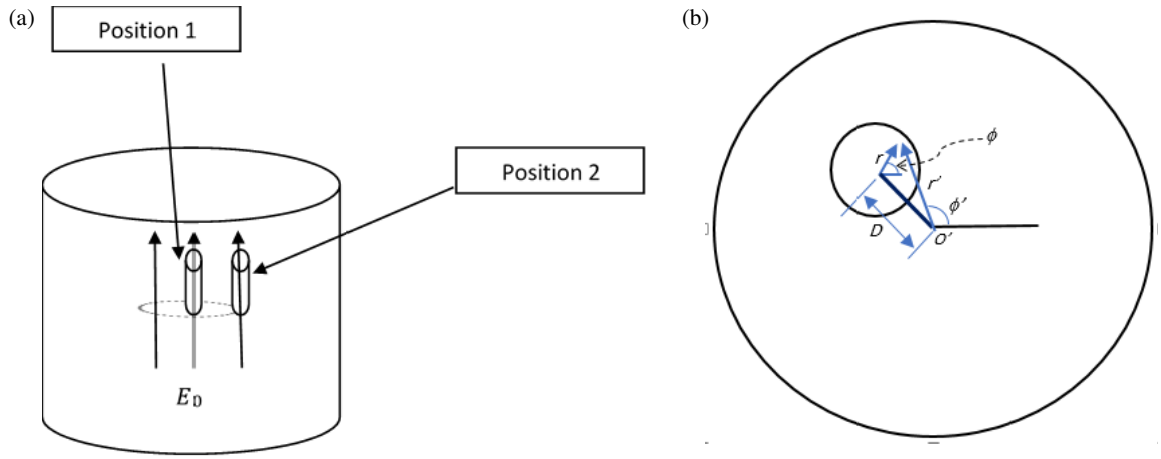

FIGURE 8. (a) Dielectric sample positions within the cavity. (b) Cylindrical coordinate transformation.

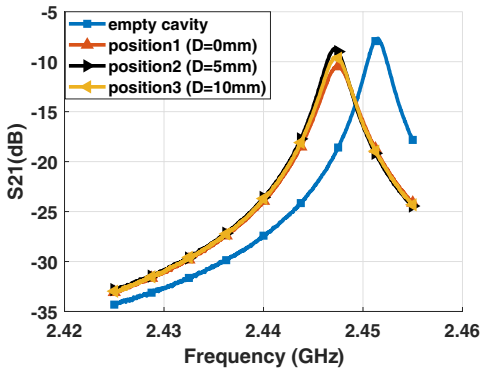

FIGURE 9. S_{21} parameters of the cavity loaded with Disk 1 at different positions.

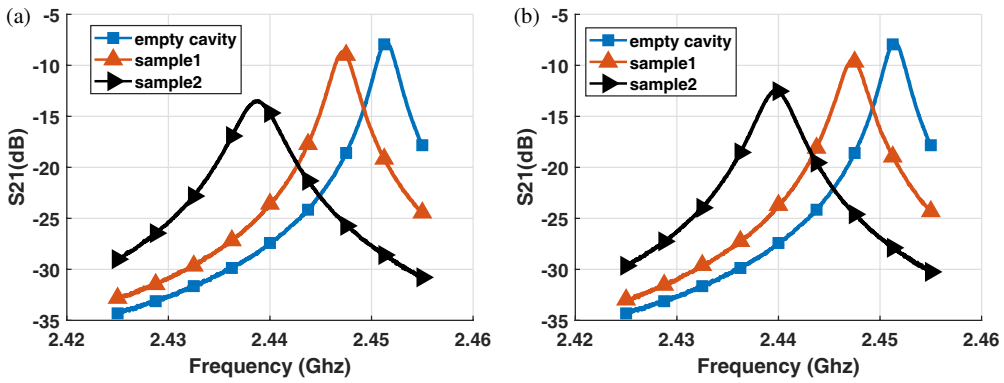

FIGURE 10. S_{21} parameters of the cavity loaded with a non-centered sample, (a) position 2 at 5 mm, (b) position 3 at 10 mm.

Overall, although the modified CPT based on the ellipsoidal or Chen's models fails to achieve accurate results for lossy, disk-shaped samples, the proposed model demonstrates notably higher accuracy in the evaluation of complex permittivity.

8. CONCLUSION

To overcome the limitations of the conventional cavity perturbation technique (CPT) and improve its accuracy in estimating the permittivity of lossy dielectrics, a more accurate account of the depolarization factor has been proposed. The focus was placed on a proposed numerical model derived from the solution of Maxwell's equations, in conjunction with the modified ellipsoidal model. The maximum sample volume was evaluated to ensure an accurate measurement of the complex permittivity. This volume depends strongly on both the sample geometry and its dielectric nature (low-loss or high-loss material). Low-loss materials present the largest sample volumes. The results were compared with those obtained using the CPT in a rectangular cavity, showing an increase in the ratio of maximum sample volume to cavity volume, with the increase exceeding 7.8%. For permittivity extraction, a comparison was performed between the proposed depolarization fac-

tor model and Chen's model. It was observed that both models yielded satisfactory results for low-loss and medium-loss materials in needle or disk geometries, whereas the ellipsoidal model showed lower accuracy. Furthermore, the proposed model exhibits superior robustness and precision in estimating the permittivity of high-loss, disk-shaped samples, whether thin or thick, compared to the ellipsoidal and Chen's models. The proposed approach can be considered reliable for accurate dielectric characterization using the cavity perturbation technique, applicable to a wide range of materials and sample shapes.

REFERENCES

[1] Jha, A. K. and M. J. Akhtar, "An improved rectangular cavity approach for measurement of complex permeability of materials," *IEEE Transactions on Instrumentation and Measurement*, Vol. 64, No. 4, 995–1003, 2015.

[2] Zinal, S. and G. Boeck, "Complex permittivity measurements using TE/sub 11p/modes in circular cylindrical cavities," *IEEE Transactions on Microwave Theory and Techniques*, Vol. 53, No. 6, 1870–1874, 2005.

[3] Seo, I. S., W. S. Chin, and D. G. Lee, "Characterization of electromagnetic properties of polymeric composite materials with free space method," *Composite Structures*, Vol. 66, No. 1–4, 533–542, 2004.

[4] Sheen, J., "Comparisons of microwave dielectric property measurements by transmission/reflection techniques and resonance techniques," *Measurement Science and Technology*, Vol. 20, No. 4, 042001, Jan. 2009.

[5] Pozar, D. M., *Microwave Engineering: Theory and Techniques*, 285–299, John Wiley & Sons, 2021.

[6] Kim, C.-K., L. Minz, and S.-O. Park, "Improved measurement method of material properties using continuous cavity perturbation without relocation," *IEEE Transactions on Instrumentation and Measurement*, Vol. 69, No. 8, 5702–5716, 2020.

[7] Jha, A. K., N. K. Tiwari, and M. J. Akhtar, "Accurate microwave cavity sensing technique for dielectric testing of arbitrary length samples," *IEEE Transactions on Instrumentation and Measurement*, Vol. 70, 1–10, 2021.

[8] Kraszewski, A. W. and S. O. Nelson, "Observations on resonant cavity perturbation by dielectric objects," *IEEE Transactions on Microwave Theory and Techniques*, Vol. 40, No. 1, 151–155, Jan. 1992.

[9] Peng, Z., J.-Y. Hwang, and M. Andriese, "Maximum sample volume for permittivity measurements by cavity perturbation technique," *IEEE Transactions on Instrumentation and Measurement*, Vol. 63, No. 2, 450–455, 2014.

[10] Parkash, A., J. K. Vaid, and A. Mansingh, "Measurement of dielectric parameters at microwave frequencies by cavity-perturbation technique," *IEEE Transactions on Microwave Theory and Techniques*, Vol. 27, No. 9, 791–795, 1979.

[11] Ghorab, K., M. L. Riabi, R. Thabet, and J. Tao, "Improved sample volume in cylindrical perturbed cavity for permittivity calculation," in *2023 22nd Mediterranean Microwave Symposium (MMS)*, 1–5, Sousse, Tunisia, 2023.

[12] Chen, D.-X., J. A. Brug, and R. B. Goldfarb, "Demagnetizing factors for cylinders," *IEEE Transactions on Magnetics*, Vol. 27, No. 4, 3601–3619, 1991.

[13] Harrison, C., "Missile with attached umbilical cable as a receiving antenna," *IEEE Transactions on Antennas and Propagation*, Vol. 11, No. 5, 587–588, 1963.

[14] Lin, M. and M. N. Afsar, "A new cavity perturbation technique for accurate measurement of dielectric parameters," in *2006 IEEE MTT-S International Microwave Symposium Digest*, 1630–1633, San Francisco, CA, USA, 2006.

[15] Jones, S. B. and S. P. Friedman, "Particle shape effects on the effective permittivity of anisotropic or isotropic media consisting of aligned or randomly oriented ellipsoidal particles," *Water Resources Research*, Vol. 36, No. 10, 2821–2833, 2000.

[16] Chen, D.-X., E. Pardo, and A. Sanchez, "Demagnetizing factors of rectangular prisms and ellipsoids," *IEEE Transactions on Magnetics*, Vol. 38, No. 4, 1742–1752, 2002.

[17] Venermo, J. and A. Sihvola, "Dielectric polarizability of circular cylinder," *Journal of Electrostatics*, Vol. 63, No. 2, 101–117, 2005.

[18] Landau, L. D. and E. M. Lifshitz, *Electrodynamics of Continuous Media*, 26, Pergamon Press, Oxford, 1960.

[19] Polaert, I., N. Benamara, J. Tao, T.-H. Vuong, M. Ferrato, and L. Estel, "Dielectric properties measurement methods for solids of high permittivities under microwave frequencies and between 20 and 250°C," *Chemical Engineering and Processing: Process Intensification*, Vol. 122, 339–345, 2017.

[20] Hutcheon, R. M., M. S. D. Jong, F. P. Adams, P. G. Lucuta, J. E. McGregor, and L. Bahen, "RF and microwave dielectric measurements to 1400°C and dielectric loss mechanisms," *MRS Online Proceedings Library (OPL)*, Vol. 269, 541, 1992.

[21] Chatterjee, A., T. Basak, and K. G. Ayappa, "Analysis of microwave sintering of ceramics," *AIChE Journal*, Vol. 44, No. 10, 2302–2311, Oct. 1998.

[22] Ghorab, K., R. Thabet, J. Tao, and M. L. Riabi, "Improvement of the perturbation technique in microwave characterization of lossy materials in a cylindrical cavity," in *19th International Conference on Microwave and High Frequency Applications (AMPERE 2023)*, Cardiff, United Kingdom, 2023.

[23] Chen, L. F., C. K. Ong, C. P. Neo, V. V. Varadan, and V. K. Varadan, *Microwave Electronics: Measurement and Materials Characterization*, John Wiley & Sons, 2004.

[24] Curtis, A. J., "Dielectric properties of polyamides: Polyhexamethylene adipamide and polyhexamethylene sebacamide," *Journal of Research of the National Bureau of Standards. Section A, Physics and chemistry*, Vol. 65A, No. 3, 185–196, 1961.